BRIEF REPORT

Indolent CD4+ CAR T-Cell Lymphoma after Cilta-cel CAR T-Cell Therapy

Metin Ozdemirli, M.D., Ph.D., Thomas M. Loughney, M.D., Emre Deniz, Ph.D., Joeffrey J. Chahine, Ph.D., Maher Albitar, M.D., Stefania Pittaluga, M.D., Sam Sadigh, M.D., Philippe Armand, M.D., Ph.D., Aykut Uren, M.D., and Kenneth C. Anderson, M.D.

SUMMARY

Indolent CD4+ cytotoxic chimeric antigen receptor (CAR) T-cell lymphoma involving the small intestine was diagnosed in a patient who had previously received ciltacabtagene autoleucel (cilta-cel) CAR T-cell therapy for treatment of myeloma. Targeted messenger RNA sequencing revealed the presence of CAR gene product in tumor cells. Whole-genome sequencing of samples of tumor and peripheral blood identified a single lentiviral insertion site within the second intron of the *SSU72* gene. In addition, numerous genetic alterations that may have contributed to malignant transformation were identified in the tumor sample. (Funded by MedStar Georgetown University Hospital.)

From the Departments of Pathology (M.O., J.J.C.) and Gastroenterology (T.M.L.), MedStar Georgetown University Hospital, and Lombardi Comprehensive Cancer Center, Georgetown University Medical Center (E.D., A.U.) — both in Washington, DC; the Genomic Testing Cooperative, Irvine, CA (M.A.); the National Institutes of Health, Bethesda, MD (S.P.); and Brigham and Women's Hospital (S.S.), the Jerome Lipper Multiple Myeloma Center, Dana–Farber Cancer Institute (K.C.A.), and Harvard Medical School (P.A.) — all in Boston. Dr. Ozdemirli can be contacted at mo7@gunet.georgetown.edu or at the Department of Pathology, MedStar Georgetown University Hospital, 3800 Reservoir Rd. NW, Washington, DC 20007.

This article was updated on June 13, 2024, at NEJM.org.

N Engl J Med 2024;390:2074-82.
DOI: 10.1056/NEJMoa2401530

Chimeric antigen receptor (CAR) T-cell therapy is an effective method of treatment for several hematologic cancers.[1] However, this therapy is associated with serious side effects, including cytokine release syndrome, prolonged cytopenias, immune effector cell–associated neurotoxicity syndrome, hemophagocytic lymphohistiocytosis–like syndrome, late neurologic toxic effects, and gastrointestinal symptoms.[2,3] Among other severe complications, rare cases of secondary T-cell lymphoma have been reported.[4-6] We describe the clinical, pathological, and molecular features of a case of an unusual gastrointestinal CD4+ cytotoxic CAR T-cell lymphoma occurring after CAR T-cell therapy. This case is notable for several reasons, including the limited extranodal tissue involvement, the morphologic and immunophenotypic resemblance to mature small T lymphocytes, the histologically indolent nature, and the CD4+ cytotoxic T-cell phenotype. Recognition of this morphologic variant and characterization of the associated molecular and genomic changes may reveal other cases and help explain the molecular mechanisms of CAR T-cell lymphomagenesis.

CASE REPORT

A 71-year-old woman with an 8-year history of multiple myeloma was treated with cyclophosphamide–fludarabine lymphodepleting therapy followed by ciltacabtagene autoleucel (cilta-cel) CAR T-cell therapy targeting B-cell maturation antigen (BCMA). She had a complete response that was negative for minimal residual disease (MRD). Four months after she had undergone CAR T-cell therapy, the patient presented with progressively worsening nonbloody diarrhea and weight loss of 5.4 kg. Her medications were intravenous immune globulin (IVIG) administered monthly and acyclovir, trimethoprim sulfamethoxazole, and rosuvastatin

taken daily. The initial laboratory assessment was remarkable for a serum bicarbonate level of 18 mmol per liter, a serum creatinine level of 1.31 mg per deciliter, a glomerular filtration rate of 44 ml per minute per 1.73 m^2 of body-surface area, a white-cell count of 5100 per cubic millimeter, a hemoglobin level of 13.7 g per deciliter, a hematocrit level of 38.1%, and a platelet count of 173,000 per cubic millimeter. The absolute neutrophil count was 4600 per cubic millimeter. The absolute lymphocyte count was 500 per cubic millimeter. Levels of liver enzymes and serum vitamin B_{12}, folic acid, C-reactive protein, iron saturation, and antienterocyte antibodies and the results of a celiac serologic panel were negative or normal. The stool calprotectin level was 6 μg per gram (normal value, <120 μg per gram). Tests of stool samples for ova and parasites, *Clostridioides difficile* antigen, strongyloides antibody, and fecal pathogen DNA analysis were all negative or normal.

The patient underwent an endoscopic examination, which revealed duodenal ulcerations. Biopsy results were interpreted as indicative of probable autoimmune enteropathy. Total parenteral nutrition was initiated. Enterography with magnetic resonance imaging and double-balloon enteroscopy revealed multiple areas of ulceration. Treatment with intravenous methylprednisolone, oral budesonide, and IVIG was initiated. With continued glucocorticoid treatment, the patient's condition improved, and glucocorticoid therapy was tapered off. After glucocorticoid therapy was discontinued, recurrent diarrhea developed. Enterography with computed tomography (CT) revealed deep ulceration in the third portion of the duodenum as well as multiple areas of mucosal hyperenhancement, most prominent in the descending colon, sigmoid colon, and distal rectum (Fig. 1A). The patient underwent deep enteroscopy and sigmoidoscopy 8 months after CAR T-cell therapy. Enteroscopy revealed a 2.5-cm clean-based ulcer with raised and firm edges in the third portion of the duodenum. Sigmoidoscopic imaging was normal in appearance. Multiple biopsy samples were obtained from the duodenal ulcer, normal duodenum, stomach, and colon for histopathological and molecular analysis.

The sample from the ulcerative mass was submitted for flow cytometric analysis. The cytospin preparation from the mass showed small lymphocytes with minimal atypia (Fig. 1B). Flow cytometric analysis revealed that 95% of the cells were T lymphocytes positive for CD2, CD3, CD5, and CD4, with 40% lacking CD7. Natural killer (NK) cells, CD8+ T cells, and CD19+ B lymphocytes made up 1% or less. Polymerase-chain-reaction (PCR) analysis of the isolated cells revealed monoclonal T-cell receptor (TCR) gene rearrangements and polyclonal immunoglobulin heavy-chain locus rearrangement, which supported the absence of MRD. A biopsy specimen of the duodenal ulcer showed villous atrophy (Fig. 1C), with a destructive small lymphocytic proliferation with minimal cytologic atypia, and numerous apoptotic bodies in the epithelium. Immunohistochemical analysis of the lymphocytes was positive for CD3, CD4, CD5, CD7 (slightly diminished), TCR-$\alpha\beta$, programmed death 1 (PD-1), B-cell lymphoma 2 (Bcl-2), granzyme B, TIA-1, and CD38. The Ki-67 proliferative index was low. CD8+ T cells, Mum-1+ plasma cells, and CD20–PAX5+ B lymphocytes were rare. In situ hybridization for Epstein–Barr virus–encoded RNA was negative.

Additional immunohistochemical analysis of random biopsy samples from the duodenum, stomach, and colon revealed small aggregates of CD4+ small T cells (Fig. 2A, 2B, and 2C). PCR analysis of these tissue blocks and random duodenum samples revealed identical biallelic clonal TCR-γ and monoclonal TCR-β gene rearrangements. These findings supported the diagnosis of indolent T-cell lymphoma and were consistent with recently described indolent T-cell lymphoma of the gastrointestinal tract.[7-9]

However, the presence of cytotoxic CD4+ T cells raised the possibility of CAR T-cell origin. The tissue paraffin block was sent for DNA and messenger RNA (mRNA) sequencing that focused on 1600 cancer-relevant genes. In brief, RNA analysis of the tumor sample revealed T-cell clonality (*TRAV5*/*TRBV19*) with more than 60% of TCR-clonality reads; a relative increase in CD4 mRNA with abnormal expression pattern; increased programmed death ligand 1, PD-1, and zeta chain–associated protein kinase 70 (ZAP70) mRNA; low-level mutations in *KMT2D* and *ERBB2* (also called *HER2*); and, most important, high levels of tumor necrosis factor receptor superfamily member 9 (TNFRSF9) CD137 (4-1BB)–CD247 (CD3ζ) and CD8A–TNFRSF9 RNA fusion. The presence of high levels of these CAR T-cell chi-

A Imaging of the Duodenum and Small Bowel

CT Enterography, Duodenal Ulcer

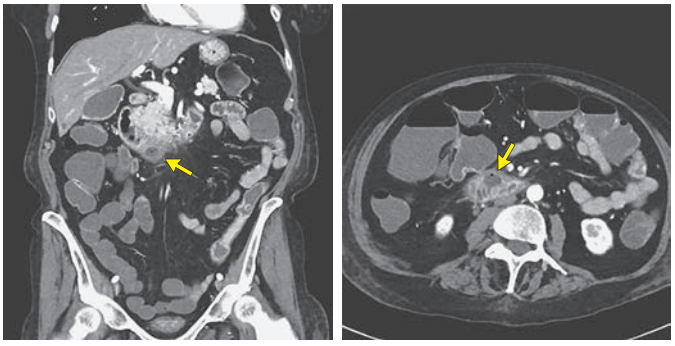

Small-Bowel Enteroscopy, Duodenal Ulcer, Third Portion

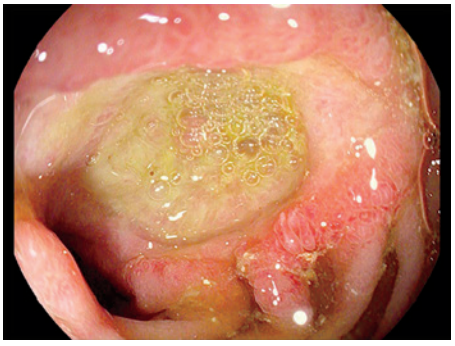

B Analysis of Ulcerative Duodenal Mass

Cytospin Analysis

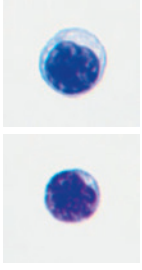

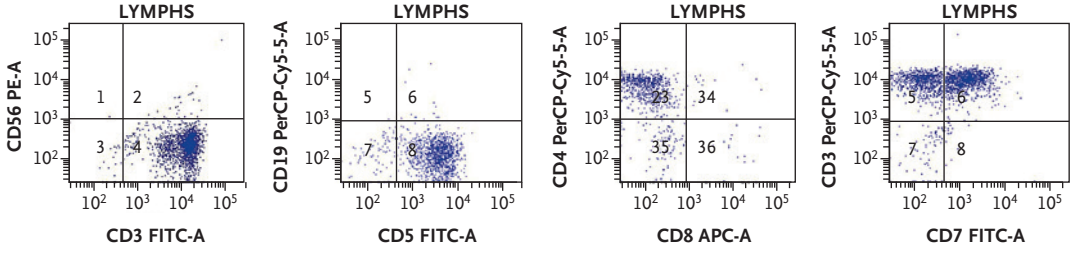

C Analysis of Ulcerative Duodenum Samples

Hematoxylin and Eosin Stain, 5×

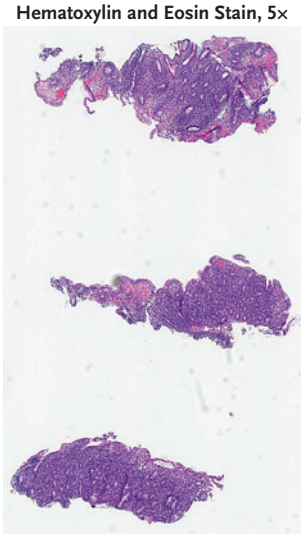

Hematoxylin and Eosin Stain, 200×

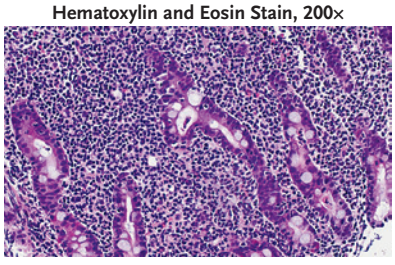

CD3, 100×

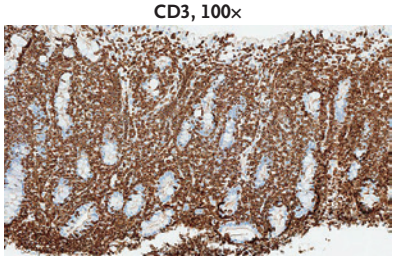

CD4, 400×

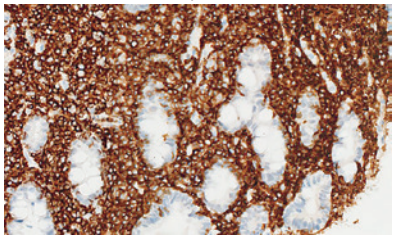

CD8, 100×

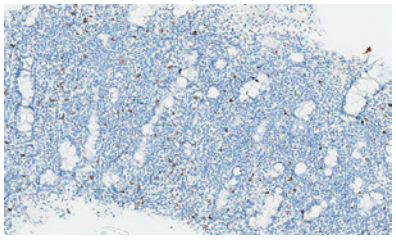

Granzyme, 200×

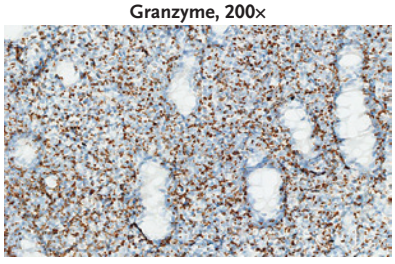

TIA-1, 200×

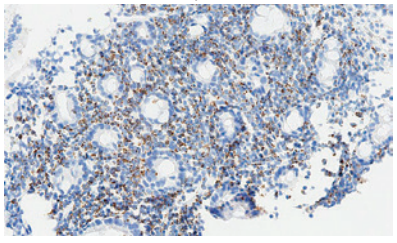

Figure 1 (facing page). Imaging and Biopsy Analyses.
Enterography with CT showed ulceration of the third portion of the duodenum with associated bowel-wall thickening and stranding of fat (Panel A, left and middle; arrows), and upper endoscopy showed a 2.5-cm ulcer with a clear base and firm and raised edges in the third portion of the duodenum (Panel A, right). Cytospin analysis of ulcerative-tissue samples with Wright–Giemsa staining revealed morphologic features representative of atypical lymphocytes (Panel B, left; original magnification, 1000×). Flow cytometric analysis of the duodenal mass cells (Panel B, right) with the use of fluorescein isothiocyanate (FITC), phycoerythrin (PE), allophycocyanin (APC), and peridinin chlorophyll protein–cyanine 5.5 (PerCP-Cy5.5) as fluorescent dyes conjugated to antibodies (A) showed 95% CD3+, CD5+, and CD4+ small T cells with partial loss of CD7. CD8+ T cells, CD56+ natural killer cells, and CD19+ B cells made up less than 1% of the cells. Sections of the duodenal-ulcer mass (Panel C, with hematoxylin and eosin staining) show an atypical small lymphoid infiltrate expanding the lamina propria with intraepithelial lymphocytes and apoptotic bodies. Immunohistochemical staining for CD3, CD4, CD8, granzyme B, and TIA-1 showed exclusively CD4+ cytotoxic T cells. Magnifications denote original magnifications.

meric fusions and the immunophenotype confirmed the presence of CD4+ CAR T cells in the tumor. On the basis of the results of this workup, a diagnosis of indolent CD4+ cytotoxic CAR T-cell lymphoma was made.

A peripheral blood sample was obtained 8 months after the patient had received CAR T-cell therapy. The possibility of donor-derived T-cell lymphoma caused by a mix-up of medicinal product was ruled out by means of HLA-DR typing. Flow cytometric analysis and PCR analysis of the peripheral-blood sample showed an identical CD4+ T-cell clone representing approximately 10% (Fig. 2E). The patient's previous intestinal-biopsy specimen (obtained 5 months after CAR T-cell therapy) was reevaluated. These analyses revealed similar morphologic and immunophenotypic findings in the duodenum and ileum as seen in the biopsies performed 8 months after CAR-T therapy (Fig. 2D). PCR analysis showed identical TCR gene rearrangements in both the 5-month and 8-month biopsy samples. In addition, next-generation sequencing of the duodenal-biopsy sample obtained 5 months after CAR-T therapy showed similar results, including findings of high levels of CAR-T fusion RNAs. A second opinion was obtained from the National Institutes of Health, where the patient had been followed previously (between 2012 and 2015, before myeloma had developed) for the presence of a minor T-cell clone associated with eosinophilia. A DNA sample was obtained from a 2015 whole-blood sample. PCR studies and next-generation sequencing for TCR gamma-chain genes of both 2015 and 2023 DNA from unsorted whole-blood samples revealed two different clonal sequences in the 2023 sample and one small clone in the 2015 sample. The 2015 sequence was different from the 2023 sequences; in addition, sequences shown in the 2023 sample were absent in the 2015 sample (up to a level of 0.001%). Both 2023 blood sequences were present in the duodenum as shown on RNA sequencing.

Staging by means of positron-emission tomography–CT did not reveal other sites of involvement. Results of bone marrow analysis were negative for T-cell infiltration.

The patient was initially treated with mycophenolate mofetil but did not have a response. She was transitioned to cyclophosphamide (50 mg orally once daily) and teduglutide (0.6 mg subcutaneously once daily) for small-bowel trophic support. Total parenteral nutrition was continued. Repeat CT enterography and enteroscopy after 7 weeks of cyclophosphamide therapy showed resolution of the duodenal ulcer. The small-bowel mucosa appeared nodular and hypertrophic. Repeat biopsies 1 year after CAR T-cell therapy revealed epithelial hypertrophy, although with persistence of lymphocytic infiltrate with morphologic characteristics and immunophenotype similar to those seen in earlier duodenal biopsy specimens (Fig. 2F) and clonal bands as shown on PCR assay that were identical to those present in earlier duodenal biopsies. As of April 2024, the patient's clinical status was slightly improved, but her diarrhea remained prominent and she continued to receive total parenteral nutrition.

MOLECULAR FINDINGS

To identify the lentiviral insertion site for the vector carrying CAR, we performed whole-genome DNA sequencing of peripheral-blood samples obtained in 2015 and 2023 and a sample of the duodenal tumor obtained 8 months after CAR T-cell therapy. The samples of duodenal tumor and 2023 blood contained an identical single insertion site. The lentiviral vector carrying the anti-BCMA CAR T-cell cassette was integrated

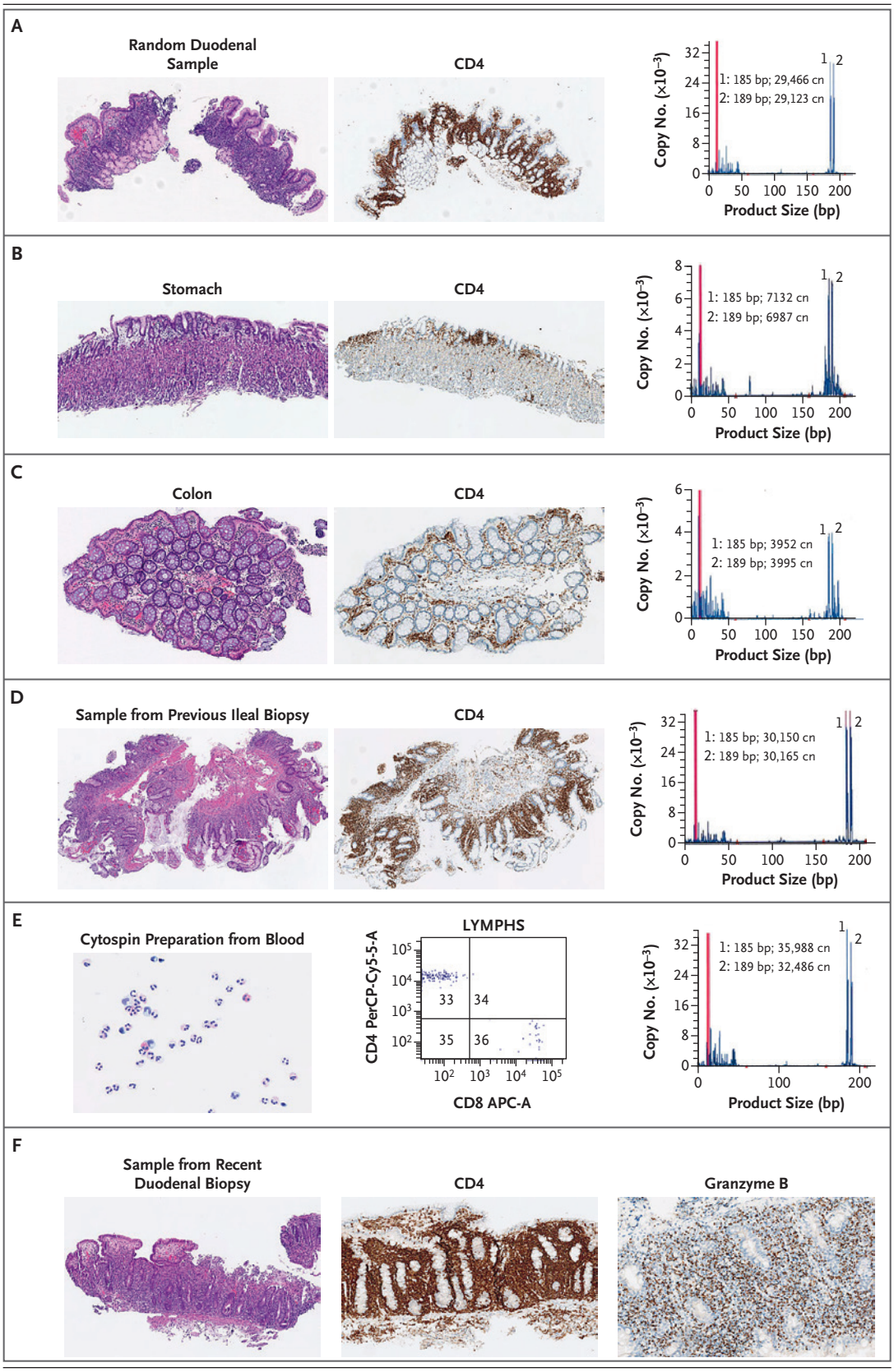

Figure 2 (facing page). Biopsy- and Blood-Sample Analyses.

Biopsy samples stained with hematoxylin and eosin (original magnification, 5×), CD4 immunostains (original magnification, 5×), and polymerase-chain-reaction (PCR) assay products (TCR gamma) are shown in Panel A (random duodenum), Panel B (stomach), Panel C (colon), and Panel D (patient's previous ileal biopsy). The analyses show destructive or subtle CD4+ monoclonal small lymphoid infiltrates, which have identical-size base-pair products (185 and 189 base pairs). In Panel E, a cytospin preparation from blood (left) shows mostly granulocytes and occasional small lymphocytes without clinically significant atypia. Flow cytometry (center) showed that 91% of lymphocytes were CD4+ T cells and 5% were CD8+ T cells. No B cells were seen. PCR assay (right) showed PCR products identical to those observed in other specimens. Panel F shows sections of recent duodenal-biopsy samples stained with hematoxylin and eosin that reveal atypical small lymphoid infiltrates with rare intraepithelial lymphocytes and apoptotic bodies (left; original magnification, 5×). The atypical cells were positive for CD4 (center; original magnification, 100×) and granzyme B (right; original magnification, 200×). The term bp denotes base pair, and cn count number.

into the positive strand of the first chromosome at position 1,556,938 (Fig. 3A and Fig. S1 in the Supplementary Appendix, available with the full text of this article at NEJM.org). The negative strand of the integration locus carried the *SSU72* gene, and the lentivirus landed within its second intron. The second allele of the *SSU72* gene was undisturbed. The corresponding locus was wild type in the 2015 blood sample. We did not observe any other genetic alterations in the *SSU72* alleles as compared with the 2015 blood sample. The exome-specific RNA sequencing of the latest duodenal-biopsy sample (obtained in January 2024) also revealed high levels of CAR T-cell fusion RNAs and showed a heterozygote polymorphism (c.399A/G) with 43% A and 57% G in the fourth exon of the *SSU72* gene, which suggests that the expression levels of the alleles were similar.

Genomic DNA sequencing of the 2015 blood sample identified multiple germline single-nucleotide polymorphisms causing start–loss or stop–gain mutations, including in *CXCR1*, *PRKD3*, and *MAP2K3* (Table S1). The total numbers of copy-number variations and structural variations with respect to genomic loci features or their types varied among the patient's samples (Fig. 3B). More than 500 somatic copy-number variations were noted, comprising at least 12,000 genes in the duodenal tumor as compared with the 2015 blood sample (Table S2). The number of somatic copy-number variations and their corresponding expression patterns, with regard to those that were available in the targeted RNA-sequencing data, were significantly correlated (Fig. 3C and Table S3). Functional annotations of the biologic pathways with the up-regulated genes of somatic copy-number–variation gains were enriched in cancer and T-cell terms (Fig. S2).

DISCUSSION

As CAR T-cell therapy becomes more commonly used for the treatment of cancers and autoimmune diseases, rarer adverse effects are likely to become more apparent, including rare secondary T-cell lymphomas. In a recent clinical trial, two cases of T-cell lymphoma were reported after allogeneic CAR T-cell therapy for lymphoma mediated with the use of PiggyBac Transposon Vector System (System Biosciences), a transposon that inserts a gene into a specific DNA site, and the trial was discontinued on that finding.[4] Recently, the Food and Drug Administration announced that it is investigating 22 cases of secondary T-cell cancer after CAR T-cell therapy, 1 of which is the present case.[5] One case of T-cell lymphoma after cilta-cel therapy was recently reported in an abstract.[6] In that patient, the neoplastic clone was identified in the apheresis product, and thus a preexisting clone had probably been driven by a combination of reported preexisting *TET2* with *JAK3* mutations and CAR T-cell therapy. A recently published study described a case of T-cell lymphoma, diagnosed 3 months after CAR T-cell therapy, that harbored the CAR transgene at very low levels, interpreted to be caused by infiltrating CAR T cells.[10] In the present case, whether the T-cell clone was already present in the infused CAR-T product is unknown, because we could not obtain a sample for testing.

Together, the observations that CAR T-cell therapies may induce clonal proliferations,[11] that there was no previous history of T-cell lymphoma or gastrointestinal symptoms, and that lymphoma developed 5 months after CAR T-cell therapy, coupled with CAR T cells and a single lentiviral insertion site within tumor cells shown 9 months after treatment, indicate that CAR T-cell therapy probably contributed to T-cell lymphomagenesis in this case.

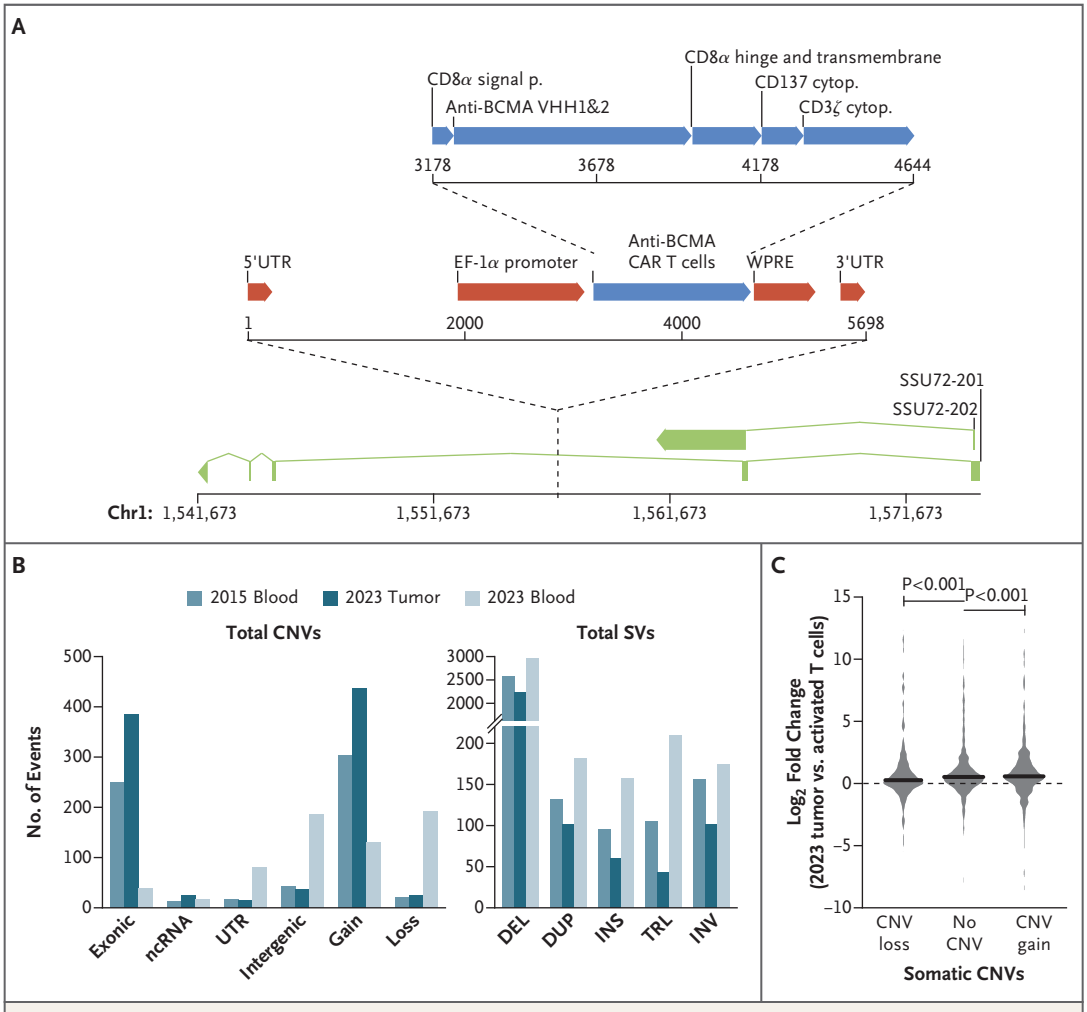

Figure 3. Genomic Integration Site of the Anti-BCMA CAR-T Lentivirus.

The anti–B-cell maturation antigen (BCMA) CAR encoding cDNA (Panel A, top of panel) was carried within a lentiviral backbone (middle of panel) that was 5698 bp long in total and included an additional random insertion of 5 nucleotides on its 3′ end at the site of the integration. According to the hg38 reference genome, at the lentiviral integration locus, the *SSU72* gene (bottom of panel) lies on the negative strand of the first chromosome between the positions of 1,541,673 and 1,574,863. *SSU72* is transcribed into either the canonical (SSU72-201) or the alternatively spliced (SSU72-202) protein coding transcripts. The canonical SSU72 transcript has 5 exons, and the start codon is located in the first exon and the stop codon is in the last exon. The lentiviral integration happened in the second intron of the gene at position 1,556,938. Blue arrows indicate the important features of the anti-BCMA CAR encoding cDNA, red arrows indicate the important features of the lentiviral backbone, and green arrows indicate the exons of the *SSU72* gene. Green lines indicate the introns of the gene. UTR denotes untranslated region and WPRE woodchuck hepatitis virus post-transcriptional regulatory element. The total numbers of copy-number variations (CNVs) (Panel B, left) and structural variations (SVs) (Panel B, right) in their functional genomic loci (exonic, intronic, noncoding [nc], untranslated region [UTR], or intergenic) or their types (gain, loss or deletion [DEL], duplication [DUP], insertion [INS], translocation [TRL], or inversion [INV]) were determined for the patient's three samples. The correlation between the CNV types (loss, no CNV, and gain) and the expression pattern of the corresponding genes in the targeted RNA sequencing (Panel C) was determined. Fold change is the ratio of the gene expression value in the 2023 duodenal tumor biopsy samples to the activated T cells. The data points are shown on a smoothed violin plot; the width of the shaded areas represents the relative number of genes with similar fold-change values, and the median of each data set is indicated by a thick horizontal line.

Among the somatic copy-number variations that had correlating expression data, multiple genes that are related to cancer or the immune system were mutated. These include proto-oncogenes *KRAS*, *MYB*, and *CBLB*; tumor-suppressors *CDKN2A*, *ATM*, and *PMS1*; receptors with their ligand pairs *HGF* and *MET*, and *NOTCH3* and *JAG2*; and genes related to immune cells, *CXCL8*, *STAT1*, and *STAT4*. These genomic alterations that were detected in the tumor sample may provide a potential explanation for how CAR T cells may have acquired or maintained the malignant phenotype.

SSU72 encodes for a phosphatase that dephosphorylates the C-terminal domain of RNA polymerase II during the termination of transcription and has indispensable roles in its regeneration and transcriptional control.[12,13] Moreover, SSU72 has essential roles for the homeostasis of CD4+ T-cell lineages.[14] By directly binding to STAT3 and ZAP70, SSU72 regulates inflammatory immune responses.[15,16] SSU72 loss halts the differentiation of regulatory T cells from CD4+ T cells by increasing effector cytokines and induces the differentiation of effector-cell lineages from activated CD4+ T cells.[17] The lentiviral CAR vector was integrated in the second intron of the *SSU72* gene in one allele, but the second allele of the *SSU72* gene remained undisrupted. The exome RNA sequencing detected intact SSU72 mRNA expression and identified a heterozygote polymorphism in exon 4. The distributions of the sequencing reads mapped to the polymorphic locus were similar, which suggests that the virus-integrated allele and the undisrupted allele had similar levels of gene expression. Therefore, the viral integration site did not appear to alter the expression level of SSU72 mRNA. In addition, an unusual splicing pattern was not observed for the *SSU72* gene. Although exome RNA sequencing may underestimate altered SSU72 mRNA products owing to its technical limitations, the data still suggest that canonical SSU72 transcript was expressed in the duodenal tumor from both alleles. Therefore, even though disruption of SSU72 expression can potentially contribute to malignant transformation of a T cell, RNA-sequencing data from the patient does not provide any evidence to support that possibility in this case.

The toxicity of CAR T-cell therapy is ascribed mainly to cytokines from effector T cells. However, activated CD4+ type 1 helper T cells possess potent Ag-dependent, major histocompatibility complex (MHC)–restricted, and cell-contact–dependent cytotoxic mechanisms[18,19] and may exhibit MHC-unrestricted cytotoxicity.[20] Thus, some of the side effects of CAR T-cell therapy may be due to direct cytotoxicity of CD4+ T cells. This case illustrates features of cell-contact cytotoxicity with intraepithelial lymphocytes and apoptotic bodies, most likely by means of granule exocytosis and FAS–FASL interactions, since high levels of perforin, granzymes, and FASL mRNA were observed in the tumor tissue by means of next-generation sequencing.

Another unusual feature of this case is the lack of clinically significant atypia or abnormal immunophenotype in the neoplastic cells and the resemblance to autoimmune enteropathy, which delayed the diagnosis. Thus, clinicians should be aware of the morphologic characteristics and immunophenotype when evaluating toxic effects of CAR T-cell therapy.

Descriptions of the treatment of indolent T-cell lymphomas of the small intestine are largely limited to case reports.[21-23] This entity does not appear to be sensitive to multiagent chemotherapy. Improvement was seen in several patients who were treated with glucocorticoids. Efficacy of treatment with cyclophosphamide, azathioprine, and other chemotherapeutic agents has not been shown. Two patients in a previous series had prompt responses to an anti-CD52 monoclonal antibody, with total clinical and histologic remission but with persistence of the neoplastic clone.[21] As of April 2024, our patient was receiving oral cyclophosphamide and teduglutide, and mild clinical, radiographic, and endoscopic improvement had been shown.[24]

We have described clinicopathological and molecular findings relative to an unusual indolent CD4+ intestinal CAR T-cell lymphoma. The addition of switch or on–off mechanisms to CAR T-cell products could possibly prevent such an unexpected, severe complication.[25,26]

Supported by the Departments of Pathology and Oncology, MedStar Georgetown University Hospital.

Disclosure forms provided by the authors are available with the full text of this article at NEJM.org.

A data sharing statement provided by the authors is available with the full text of this article at NEJM.org.

We thank the patient, who gave consent for the study; Nicole Mueller and James Doan for technical assistance; and Elaine S. Jaffe for providing the 2015 blood DNA sample and reading the initial version of the manuscript.

REFERENCES

1. Jogalekar MP, Rajendran RL, Khan F, Dmello C, Gangadaran P, Ahn BC. CAR T-cell-based gene therapy for cancers: new perspectives, challenges, and clinical developments. Front Immunol 2022;13:925985.
2. Mucha SR, Rajendram P. Management and prevention of cellular-therapy-related toxicity: early and late complications. Curr Oncol 2023;30:5003-23.
3. Abu-Sbeih H, Tang T, Ali FS, et al. Gastrointestinal adverse events observed after chimeric antigen receptor T-cell therapy. Am J Clin Oncol 2019;42:789-96.
4. Micklethwaite KP, Gowrishankar K, Gloss BS, et al. Investigation of product-derived lymphoma following infusion of piggyBac-modified CD19 chimeric antigen receptor T cells. Blood 2021;138:1391-405.
5. Verdun N, Marks P. Secondary cancers after chimeric antigen receptor T-cell therapy. N Engl J Med 2024;390:584-6.
6. Harrison SJ, Nguyen T, Rahman M, et al. CAR+ T-cell lymphoma post ciltacabtagene autoleucel therapy for relapsed refractory multiple myeloma. Blood 2023;142:Suppl 1:6939 (https://ashpublications.org/blood/article/142/Supplement%201/6939/504399/CAR-T-Cell-Lymphoma-Post-Ciltacabtagene-Autoleucel).
7. Swerdlow SH, Campo E, Pileri SA, et al. The 2016 revision of the World Health Organization classification of lymphoid neoplasms. Blood 2016;127:2375-90.
8. Carbonnel F, d'Almagne H, Lavergne A, et al. The clinicopathological features of extensive small intestinal CD4 T cell infiltration. Gut 1999;45:662-7.
9. Soderquist CR, Patel N, Murty VV, et al. Genetic and phenotypic characterization of indolent T-cell lymphoproliferative disorders of the gastrointestinal tract. Haematologica 2020;105:1895-906.
10. Ghilardi G, Fraietta JA, Gerson JN, et al. T cell lymphoma and secondary primary malignancy risk after commercial CAR T cell therapy. Nat Med 2024 January 24 (Epub ahead of print).
11. Shah NN, Qin H, Yates B, et al. Clonal expansion of CAR T cells harboring lentivector integration in the CBL gene following anti-CD22 CAR T-cell therapy. Blood Adv 2019;3:2317-22.
12. Krishnamurthy S, He X, Reyes-Reyes M, Moore C, Hampsey M. Ssu72 is an RNA polymerase II CTD phosphatase. Mol Cell 2004;14:387-94.
13. Hwang S, Kim MH, Lee CW. Ssu72 dual-specific protein phosphatase: from gene to diseases. Int J Mol Sci 2021;22:3791.
14. Kim MH, Lee CW. Phosphatase Ssu72 is essential for homeostatic balance between CD4+ T cell lineages. Immune Netw 2023;23:e12.
15. Lee SH, Kim EK, Kwon JE, et al. Ssu72 attenuates autoimmune arthritis via targeting of STAT3 signaling and Th17 activation. Sci Rep 2017;7:5506.
16. Ko JS, Jeong D, Koh J, et al. Ssu72 phosphatase directly binds to ZAP-70, thereby providing fine-tuning of TCR signaling and preventing spontaneous inflammation. Proc Natl Acad Sci U S A 2021;118(35):e2102374118.
17. Lee JK, Koo SY, Nam HM, et al. Ssu72 is a T-cell receptor-responsive modifier that is indispensable for regulatory T cells. Cell Mol Immunol 2021;18:1395-411.
18. Ozdemirli M, el-Khatib M, Bastiani L, Akdeniz H, Kuchroo V, Ju ST. The cytotoxic process of CD4 Th1 clones. J Immunol 1992;149:1889-95.
19. Ju ST, Matsui K, Ozdemirli M. Molecular and cellular mechanisms regulating T and B cell apoptosis through Fas/FasL interaction. Int Rev Immunol 1999;18:485-513.
20. Ozdemirli M, Akdeniz H, el-Khatib M, Ju ST. A novel cytotoxicity of CD4+ Th1 clones on heat-shocked tumor targets. I. Implications for internal disintegration model for target death and hyperthermia treatment of cancers. J Immunol 1991;147:4027-34.
21. Malamut G, Meresse B, Kaltenbach S, et al. Small intestinal CD4+ T-cell lymphoma is a heterogenous entity with common pathology features. Clin Gastroenterol Hepatol 2014;12:599-608.e1.
22. Fan W, Niu L, He H, et al. Indolent T-cell lymphoproliferative disorder of gastrointestinal tract with unusual clinical courses: report of 6 cases and literature review. Virchows Arch 2023;482:729-43.
23. Liu H, Cao L, Zhao X, et al. Metronomic chemotherapy for indolent T-cell lymphoproliferative disorder of the gastrointestinal tract. Cancer Sci 2023;114:3793-6.
24. Schwartz LK, O'Keefe SJ, Fujioka K, et al. Long-term teduglutide for the treatment of patients with intestinal failure associated with short bowel syndrome. Clin Transl Gastroenterol 2016;7:e142.
25. Stock S, Klüver AK, Fertig L, et al. Mechanisms and strategies for safe chimeric antigen receptor T-cell activity control. Int J Cancer 2023;153:1706-25.
26. Kvorjak M, Ruffo E, Tivon Y, et al. Conditional control of universal CAR T cells by cleavable OFF-switch adaptors. ACS Synth Biol 2023;12:2996-3007.